

Article

A Novel Insensitive Cocrystal Explosive Composed of BTF and the Non-Energetic 2-Nitroaniline

Sijia Du ¹, Yunshu Zhao ², Yapeng Ou ^{1,*} , Zijie Bi ¹, Shanhu Sun ^{2,*} and Tao Yan ³¹ School of Mechatronic Engineering, Beijing Institute of Technology, Beijing 100081, China² Analysis and Testing Center, Southwest University of Science and Technology, Mianyang 621010, China³ College of Aerospace and Civil Engineering, Harbin Engineering University, Harbin 150001, China

* Correspondence: ouyapeng@bit.edu.cn (Y.O.); shanhushun@swust.edu.cn (S.S.)

Abstract: Benzotrifuroxan (BTF) is a powerful energetic material (EM) with high density that can be used both as a primary and a secondary explosive. However, high mechanical sensitivity limits its application prospects. To actualize its potential, cocrystallization was introduced into BTF-based EMs for insensitivity improvement in the current work. A novel cocrystal explosive composed of BTF and a non-energetic molecule (2-Nitroaniline (ONA)) was prepared with a molar ratio of 1:1. The possible mechanism of cocrystal formation was studied by the analysis and characterization of its crystal structure, and the crystal structure, thermal decomposition, and energetic properties were investigated. The results indicate that the formation of the BTF/ONA cocrystal is mainly attributed to the strong interactions of the hydrogen bonds formed between the hydrogen on the amino group in the ONA molecule and the oxygen and nitrogen atoms in BTF. The impact sensitivity of BTF/ONA is obviously reduced, with the drop height of 50% explosion probability (H_{50}) increasing from 56.0 to 90.0 cm. The calculated detonation velocity and detonation pressure of the BTF/ONA cocrystal are 7115.26 m/s and 20.51 GPa, respectively. The decomposition peak temperature of the BTF/ONA cocrystal (191.1 °C) decreases by about 90.9 °C compared to BTF (282.0 °C). This suggests that cocrystallization could effectively reduce its impact sensitivity and produce an explosive with excellent comprehensive properties.

Keywords: benzotrifuroxan; cocrystallization; energetic materials; mechanical sensitivity



Citation: Du, S.; Zhao, Y.; Ou, Y.; Bi, Z.; Sun, S.; Yan, T. A Novel Insensitive Cocrystal Explosive Composed of BTF and the Non-Energetic 2-Nitroaniline. *Crystals* **2024**, *14*, 722. <https://doi.org/10.3390/cryst14080722>

Academic Editor: Cristóbal Verdugo-Escamilla

Received: 13 July 2024

Revised: 9 August 2024

Accepted: 11 August 2024

Published: 13 August 2024



Copyright: © 2024 by the authors. Licensee MDPI, Basel, Switzerland. This article is an open access article distributed under the terms and conditions of the Creative Commons Attribution (CC BY) license (<https://creativecommons.org/licenses/by/4.0/>).

1. Introduction

An explosive is a reactive substance that contains a great deal of energy that can instantly release heat and a large amount of gas when appropriately stimulated [1]. It is widely used as a source of energy for weapons and spacecraft [2,3]. With the pursuit of miniaturization, higher rates of fire, and high destructive capabilities in advanced weapons, the development and application of high-energy-density materials (HEDMs) have become key research areas in the field of energetic materials (EMs) [4–7]. Still, there is usually a contradictory relationship between energy density and the safety of explosives. Research on the desensitization of HEDMs is particularly important [8]. Currently, the main methods of insensitive improvement include the surface coating of insensitive materials, sphericalization, nanosizing, and cocrystallization [9–13]. Among them, cocrystallization is a strategy that modifies the properties of EMs at the molecular level without altering the molecular structure of explosives. It involves stabilizing explosive molecules with other compounds through non-covalent bonds like hydrogen bonds, van der Waals forces, or π - π interactions within the same crystal lattice [14]. Therefore, cocrystallization creates a unique crystal structure and achieves more comprehensive and balanced properties [15,16]. By adjusting the components and proportions of the cocrystal formers, it is possible to control the mechanical sensitivity precisely, optimizing their explosive performance and achieving a high degree of suitability for specific applications. In 2011, the CL-20/TNT cocrystal

yielded a significant reduction in impact sensitivity compared to any polymorph of CL-20 [17]. In 2012, Adam J. Matzger et al. [18] prepared a 2,4,6,8,10,12-hexanitro-2,4,6,8,10,12-hexaazaisowurtzitane (CL-20)/1,3,5,7-tetranitro-1,3,5,7-tetrazocane (HMX) cocrystal, which reduced the mechanical sensitivity of CL-20 without significantly lowering its denotation performance. These indicate that cocrystallization is an effective method for reducing the mechanical sensitivity of HEDMs.

Benzotrifuroxan (BTF) is an ideal oxygen-balanced hydrogen-free explosive with three furoxan rings and no nitro groups [19]. It exhibits excellent detonation performance and can be used both as a primary explosive and a secondary explosive [20]. Its density is nearly 1.9 g/cm^3 , and its thermal stability and detonation performance are comparable to HMX [21,22]. However, BTF's high mechanical sensitivity limits its application prospects [20,23]. Interestingly, BTF shows the potential to form cocrystals with other compounds because the strong polarizing effects of the oxygen and nitrogen atoms in the BTF molecule cause interactions with compounds relatively rich in electron density due to nitro groups [15]. According to the report, many novel BTF cocrystals were prepared, including BTF/3,4-Dinitrofurazanfuroxan (DNTF) [24], BTF/2,4,6-trinitrotoluene (TNT) [25], BTF/1,3,5-trinitrobenzene (TNB), BTF/2,4,6-trinitroaniline (TNA), BTF/2,4,6-trinitrobenzene methylamine (MATNB), 1,3,3-trinitroazetidine (TNAZ), and BTF/CL-20 [26]. Among them, the energetic cocrystal constructed by BTF and aromatic nitro compounds such as TNT and TNB can more effectively reduce its mechanical sensitivity. The six-membered ring of BTF consists of an electron-poor π -system, so theoretically, BTF could have a higher chance of obtaining cocrystals with partner compounds containing a higher number of electron-rich groups, such as nitrobenzene [27].

The increase in molecular stability enables the realization of their insensitivity enhancement. Here, aromatic nitro compounds and nitramine were considered to be ideal energetic materials that could offer predictable hydrogen-bonding and π -stacking interactions for HEDMs. The molecular stability increases with the increase in the NH_2 group, which offers more conjugated π -electrons and intermolecular and intramolecular hydrogen bonds [8]. In the current work, the aromatic nitro and nitramine compound 2-Nitroaniline (ONA) was screened as the conformer molecule of BTF, and a BTF/ONA cocrystal with a molecular ratio of 1:1 was successfully prepared by solvent volatilization. This study introduces the cocrystal structure, thermal properties, and denotation performance of the BTF/ONA cocrystal. It aims to produce an explosive with excellent comprehensive properties and provide insights for the design of BTF cocrystals.

2. Experimental Section

2.1. Materials and Sample Preparation

BTF ($\text{C}_6\text{N}_6\text{O}_6$) was synthesized using 5,7-dichloro-4,6-dinitrobenzofuran and sodium azide. The reaction of 5,7-dichloro-4,6-dinitrobenzofuran with sodium azide in a 1:2 ratio was carried out at low temperatures in an acetone/water mixture [28]. ONA ($\text{C}_6\text{H}_6\text{N}_2\text{O}_2$) and acetone ($\text{C}_3\text{H}_6\text{O}$) were provided by Shanghai Meirui Biochemical Technology Co., Ltd. The BTF sample was characterized using High-Performance Liquid Chromatography (HPLC), and the results are shown in SI 1. HPLC assay results show that the purity of BTF in the synthesized sample is 99.73%. Figure 1 shows the molecular structures of BTF and ONA.

In a typical process of cocrystallization, BTF (25.21 mg, 0.1 mmol) and ONA (13.81 mg, 0.1 mmol) were completely dissolved in a 10 mL acetone solvent under stirring. The mixture was then left to crystallize in a Thermo Scientific oven (Waltham, MA, USA) for 72 h. Temperature was constantly $25\sim 30 \text{ }^\circ\text{C}$, and relative humidity was 60~70%. The solvent slowly evaporated at room temperature, resulting in the formation of a new 1:1-molar-ratio BTF/ONA cocrystal explosive.

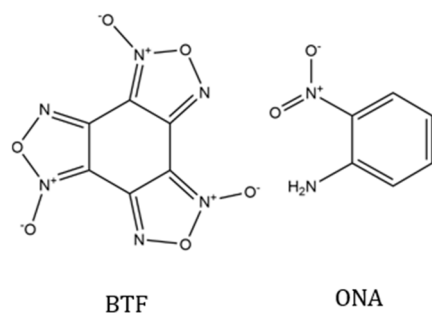


Figure 1. Molecular structures of BTF and ONA.

2.2. Characterization

The cocrystal of BTF and ONA was characterized using several techniques to determine its structure and properties.

A SuperNova Dual, Cu at zero, AtlasS2 diffractometer (Palo Alto, CA, USA) was used for Single-Crystal X-ray Diffraction (SXRD) with Cu K α X-ray source ($\lambda = 1.54184 \text{ \AA}$) and ω -scans. A single crystal of suitable quality was chosen and purged with a cooled nitrogen gas stream at 100.00 K throughout the data collection. Collected data were integrated with CrysAlis Pro software (1.171.38.43f; Rigaku Oxford Diffraction 2015). CrysAlisPro 1.171.38.43f was used for the empirical absorption correction, which was implemented using spherical harmonics in the SCALE3 ABSPACK scaling algorithm. The structures were solved using ShelXT software (Sheldrick, 2015), and the solutions were refined using ShelXL software (Sheldrick, 2015). The analyses of SXRD data were carried out using the OLEX2 program.

A PANalytical Empyrean intelligent diffractometer (Almelo, Netherlands) was used for Powder X-ray Diffraction (PXRD) at room temperature, utilizing Cu-K α radiation ($\lambda = 1.54056 \text{ \AA}$, $I = 30 \text{ mA}$, $U = 40 \text{ kV}$). The sample was placed onto a glass circular sample holder and aligned with a glass slide. Scans were conducted according to the following parameters: $2\theta = 5^\circ$ to 60° , step size = 0.033° , and step speed = 0.2 s .

A Fourier–transform infrared spectrometer (Shimadzu FTIR 8400s, Kyoto, Japan) was used for Infrared Spectroscopy (IR). Approximately 1–2 mg of the sample was mixed with 180 mg of KBr particles. The mixture was triturated in an agate mortar and pressed into a slice of KBr with the sample in a mole. The infrared spectra were collected in the range of 500 to 4000 cm^{-1} with a resolution of 2 cm^{-1} .

The thermal properties of the cocrystalline compound were measured by Differential Scanning Calorimetry (DSC) using a METTLER TOLEDO TGA/DSC 3+ instrument (Nänikon, Switzerland). The BTF/ONA cocrystal explosive samples were manually ground into a fine powder. Approximately 1–2 mg of the sample was placed in an alumina crucible (Beijing, China). The sample was heated from $30 \text{ }^\circ\text{C}$ to $450 \text{ }^\circ\text{C}$ at a rate of 20 K/min under a pure nitrogen atmosphere (50 mL/min).

The sensitivity was measured using a WL-1-type impact sensitivity instrument with a 2.5 kg drop weight, according to the Chinese GJB-772A-97 standard method 601.2 [29].

3. Results and Discussion

3.1. Single–Crystal X-ray Diffraction of BTF/ONA

The crystallographic data and structure refinement parameters are listed in Table S1. They show that BTF/ONA belongs to a monoclinic crystal system and the $P2_1/n$ space group with lattice parameters of $Z = 4$ and $a = 13.6285(4) \text{ \AA}$, $b = 13.8193(3) \text{ \AA}$, $c = 16.0688(4) \text{ \AA}$, $\alpha = 90.00^\circ$, $\beta = 101.786(3)^\circ$, $\gamma = 90.00^\circ$, and $V = 2962.53(13) \text{ \AA}^3$. Figure 2a is a simulated packing of the BTF/ONA cocrystal. Figure 2b shows the geometry of molecules in anisotropic ellipsoids.

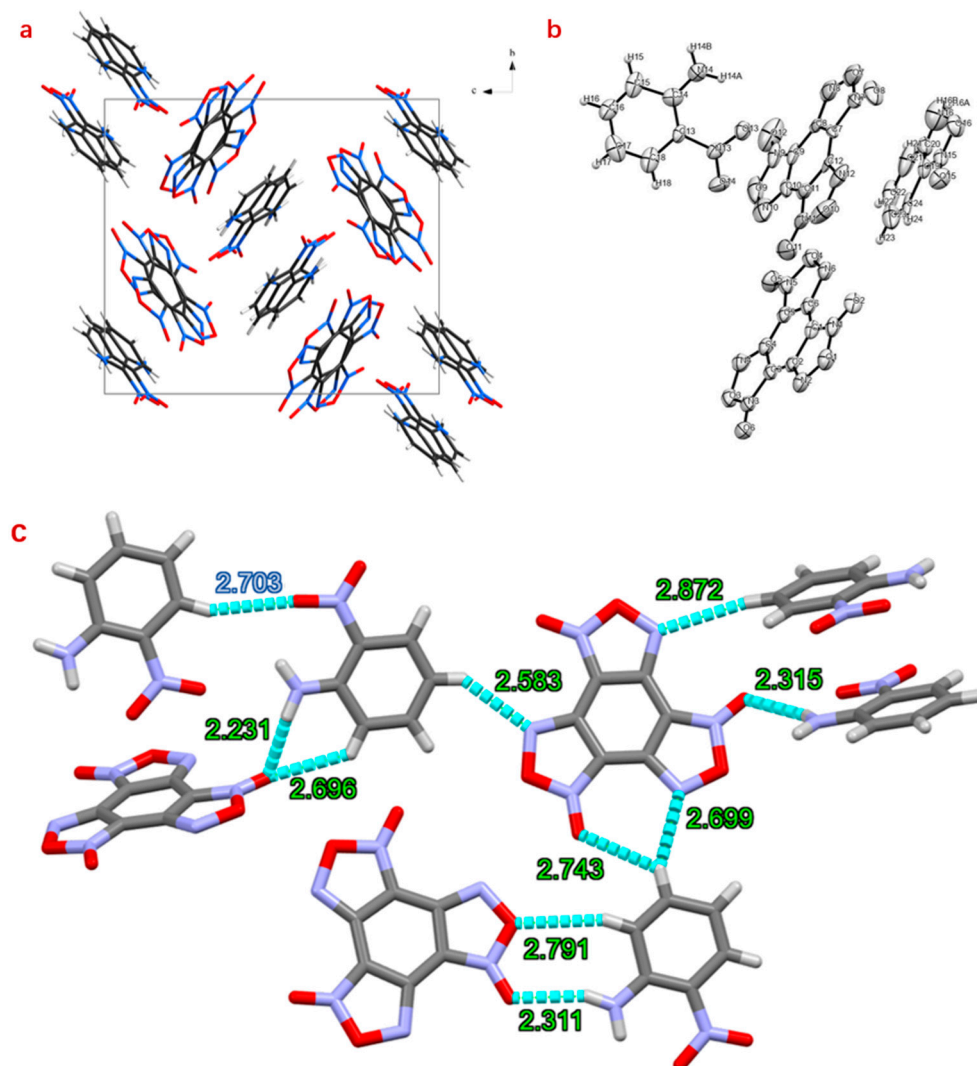


Figure 2. (a) Simulated packing of the BTF/ONA cocrystal; (b) OPTEP diagram for BTF/ONA cocrystal with 50% probability ellipsoids; (c) hydrogen-bonding interactions between BTF and ONA. The green numbers are hydrogen bond distances for BTF-ONA and the blue number is hydrogen bond distances for ONA-ONA.

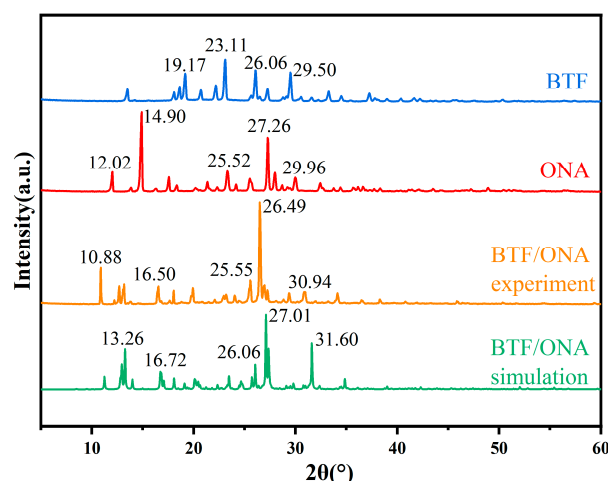
Its asymmetric unit consists of one BTF molecule and one ONA molecule. The structure of the BTF cocrystals is stabilized mainly through hydrogen-bonding and π -stacking interactions [25]. By analyzing the relative contributions of various intermolecular interactions, it is found that the hydrogen bond may play a very important role in the crystal structure of the BTF/ONA cocrystal. The possible hydrogen bond distances and angles are shown in Figure 2c and listed in Table 1. They imply that a large number of intermolecular hydrogen bonds are distributed between the BTF and its conformer molecules. Figure 2c shows that three strong interactions of $N_{16}-H_{16B}\cdots O_{11}$ (2.231 Å, 146.92°), $N_{16}-H_{16B}\cdots O_{11}$ (2.311 Å, 155.16°), and $N_{14}-H_{14A}\cdots O_6$ (2.315 Å, 146.61°) were formed between the hydrogen on the amino group in the ONA molecule and the oxygen and nitrogen atoms in BTF. In addition, a weaker hydrogen bond appears between adjacent ONA molecules. For example, the hydrogen bond of $N_{18}-H_{18}\cdots O_{16}$ (2.703 Å, 152.56°) occurred between two adjacent ONA molecules. These hydrogen bonds were considered to be the main driving force for the formation and stabilization of the BTF/ONA cocrystal.

Table 1. Hydrogen bonding of BTF–ONA cocrystal.

	D–H...A	D (H...A)/Å	∠DHA/°
BTF–ONA	C ₁₇ –H ₁₇ ...N ₂	2.872	166.61
	C ₂₃ –H ₂₃ ...N ₆	2.583	137.32
	N ₁₄ –H _{14A} ...O ₆	2.315	146.41
	C ₁₆ –H ₁₆ ...N ₄	2.699	141.99
	C ₁₆ –H ₁₆ ...O ₅	2.743	217.10
	N ₁₄ –H _{14B} ...O ₈	2.311	155.16
	C ₁₅ –H ₁₅ ...O ₇	2.791	153.07
	C ₂₁ –H ₂₁ ...O ₁₁	2.696	128.67
	N ₁₆ –H _{16B} ...O ₁₁	2.231	146.92
ONA–ONA	N ₁₈ –H ₁₈ ...O ₁₆	2.703	152.56

3.2. Cocrystal Structure and Characteristics of BTF/ONA

To examine the crystalline phase and purity of the cocrystal, PXRD and IR analyses were carried out. The corresponding PXRD patterns are shown in Figure 3, and the observed results from PXRD at room temperature are summarized in Table S2. The PXRD pattern of the BTF/ONA cocrystal is distinctly different from those of the individual components, BTF and ONA. The characteristic peaks of BTF/ONA are observed at 10.88°, 16.50°, 25.55°, 26.49°, and 30.94°. The experimental pattern was nicely comparable to simulated PXRD patterns, which were calculated from crystal structures using Mercury software (22.01.8). The small differences in intensity were due to the preferred orientation of crystalline particles [30]. Moreover, it showed small temperature-dependent shifts in the peak positions (PXRD at RT and SXRD crystal data at 100 K) [31]. The lower temperatures at which SXRD was measured caused the lattice to shrink and the characteristic peaks to be shifted toward higher degree numbers. The characteristic peaks of BTF appeared at 19.17°, 23.11°, 26.06°, and 29.50°, and the characteristic peaks of ONA appeared at 12.02°, 14.90°, 25.52°, 27.26°, and 29.96°. Overall, the BTF/ONA cocrystal showed different crystalline phases with the appearance of new characteristic peaks in the PXRD patterns. The above results indicate that a new crystalline phase composed of BTF and ONA was successfully formed.

**Figure 3.** PXRD patterns for BTF, ONA, and the BTF/ONA cocrystal.

The IR spectra of BTF, ONA, and the BTF/ONA cocrystal are shown in Figure 4, and their related data are summarized in Table S3. BTF is a furoxan compound, while ONA is a nitroaniline compound. The characteristic absorption peak due to the C–H stretching vibration in ONA appears at 3102.9 cm^{−1}, and the corresponding characteristic absorption peaks of the amine groups in BTF/ONA appear at 3491.0 cm^{−1} and 3384.5 cm^{−1}.

However, compared to both, the hydroxyl group position of BTF/ONA has changed. A strong bond attributed to the C=N stretching vibration in the furan structure is observed at about 1656 cm^{-1} . BTF has a peak at 1657.3 cm^{-1} , and the BTF/ONA cocrystal has a peak at 1649.8 cm^{-1} , indicating a shift in the peak of the BTF/ONA cocrystal. The above absorption peaks are consistent with the results reported in previous works [32]. In the low wavenumber range, Figure 4 shows that some peaks of the individual components disappear or shift significantly in the cocrystal infrared spectrum, such as the peak of BTF at 961.8 cm^{-1} and the peak of ONA at 1341.7 cm^{-1} . The changes in peak positions and intensities in the spectra for BTF, ONA, and the BTF/ONA cocrystals indicate interactions between the two individual components, leading to the formation of a new crystal structure.

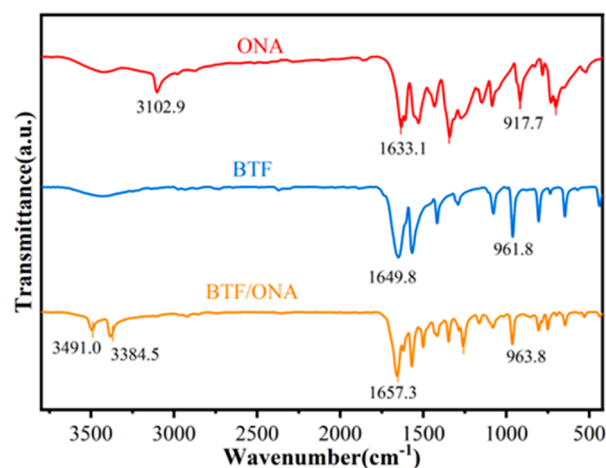


Figure 4. IR spectra for BTF, ONA, and the BTF/ONA cocrystal.

3.3. Detonation Performances and Sensitivity of BTA/ONA

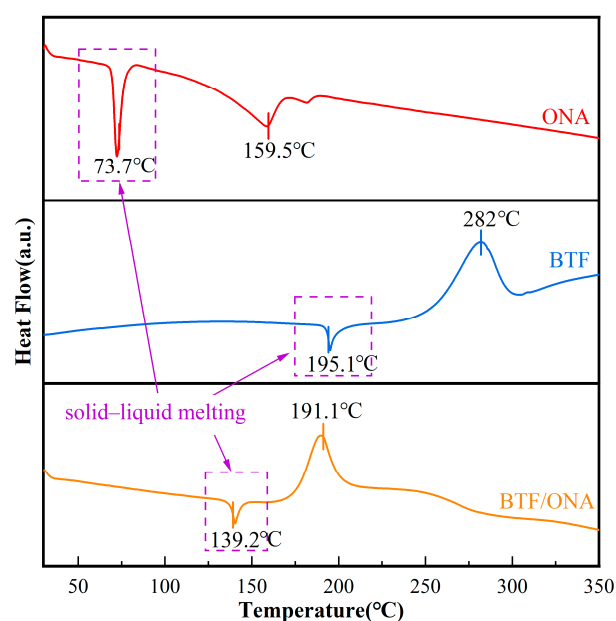
A summary of the data and results of the detonation performances and the impact sensitivity study of BTF and the BTF/ONA cocrystal is shown in Table 2. For a detailed evaluation of the influence of cocrystallization on the detonation properties, the enthalpy of formation was calculated. The detonation properties for the BTF/ONA cocrystal and BTF, including detonation velocity and detonation pressure at theoretical maximum density (TMD), were calculated using *Explo5*. Cocrystallization can produce some changes in important physical properties of energetic materials, such as density, which is a decisive factor for detonation properties [33]. The detonation velocity of the BTF/ONA cocrystal is 7115.26 m/s , and the detonation pressure is 20.51 GPa , which is lower than that of BTF. This is probably attributed to the cocrystallization of BTF with the non-energetic ONA molecule, which decreases the density and increases the heat of formation, thereby lowering the energy density [22]. Cocrystallization enhances the intermolecular binding force, decreases the molecular packing density, reduces the density, and deteriorates the oxygen balance, leading to a reduction in the detonation performance [34]. The 50% drop height reflecting the impact sensitivity of the BTF/ONA cocrystal is 90 cm , which is significantly higher than that of pure BTF (56 cm). The measured impact sensitivity is greatly reduced. The sensitivity and explosion performance greatly depend on the intermolecular interactions, chemical composition, and molecular spatial packing density of the explosive [30]. All in all, BTF/ONA has a significantly higher drop height and slightly lower detonation velocity and detonation pressure than BTF. This indicates that forming a cocrystal with non-energetic molecules can effectively alter impact sensitivity and further enhance the safety of sensitive energetic materials. In order to balance safety and energy, non-energetic nitrobenzenes are a better option to synthesize BTF cocrystals for a wider range of applications.

Table 2. Energetic properties for BTF, ONA, and the BTF/ONA cocrystal.

	BTF/ONA	BTF
Formula	$C_{12}N_8O_{12}H_6$	$C_6N_6O_6$
Oxygen balance	−77.9%	−38.1%
MW [$g\ mol^{-1}$]	390.263	252.103
Density [$g\cdot cm^{-3}$]	1.656	1.87
Enthalpy of formation [$kJ\ mol^{-1}$]	721.21	671.78
Detonation velocity [$m\ s^{-1}$]	7115.26	8959.98
Detonation pressure [GPa]	20.51	36.35
$H_{50\%}$ [cm]	90	54

3.4. Thermal Properties of BTF/ONA

To make a comparison of thermal properties, the BTF/ONA cocrystal and the pure individual components were analyzed using DSC, and the data are shown in Figure 5. A clear endothermic peak at 195.1 °C in the BTF crystal corresponds to the solid–liquid phase transition of the melting process before thermal decomposition [33]. The melting point of ONA is near 73.7 °C. Meanwhile, the melting point of the BTF/ONA cocrystal is 139.2 °C, which is between those of BTF and ONA. The DSC curves of BTF/ONA and BTF have exothermic peaks. Both the initial decomposition temperature (176 °C) and the exothermic peak temperature (191.1 °C) of the cocrystal shift to lower temperatures compared to BTF. Meanwhile, the curve of BTF/ONA shows a subsequent main exothermic peak and a shoulder exothermic peak at a higher temperature. The above results imply that the thermal stability of the cocrystal under the same heating conditions is between BTF and ONA. The melting points of ONA and TNT are similar, as are those of BTF/ONA and BTF/TNT (132.6 °C) [25]. The differing thermal behavior may have resulted from the changing lattice energies of the cocrystals and cofomers [35]. Moreover, the curve of ONA does not have a completed decomposition peak, mainly attributed to sublimation after melting under heating. The lower melting point and the absorption of heat by non-energy-containing molecules could be the reason for the decrease in the detonation performances of the BTF/ONA cocrystal.

**Figure 5.** DSC curves for BTF, ONA, and the BTF/ONA cocrystal.

4. Conclusions

Here, a novel cocrystal explosive composed of BTF and the non-energetic molecule ONA in a molar ratio of 1:1 is presented, demonstrating the application of cocrystallization as a strategy for realizing enhanced insensitivity of explosives. The formation of the BTF/ONA cocrystal is mainly attributed to the strong interactions of the hydrogen bonds formed between the hydrogen on the amino group in the ONA molecule and the oxygen and nitrogen atoms in BTF. The cocrystal structure, thermal stability, detonation performances, and mechanical sensitivity of BTF/ONA were investigated. A comparison of the PXRD patterns and IR spectra of the cocrystal with those of the individual components indicates significant changes in cocrystal structure. These results suggest the formation of a new molecular cocrystal. Meanwhile, this is also evidenced by a significant shift in the endothermic peak of the decomposition of the cocrystal (191.1 °C) to the low-temperature region in comparison with the BTF (282.0 °C). The calculated detonation velocity of the BTF/ONA cocrystal is 7115.26 m/s, and the detonation pressure is 20.51 GPa. The cocrystallization of BTF with ONA changes thermal properties and slightly reduces detonation performance. The BTF/ONA cocrystal has a 50% drop height of 90 cm, decreased by about 60%. It affords a tremendous reduction in impact sensitivity in comparison to pure BTF. The viability of BTF in explosive applications is potentially improved. This paper poses an important consideration in the design of future BTF and other explosive cocrystals, especially with non-energetic molecules such as nitroaniline.

Supplementary Materials: The following supporting information can be downloaded at <https://www.mdpi.com/article/10.3390/cryst14080722/s1>: Figure S1: Chromatogram; Table S1: Accumulated points of chromatogram; Table S2: Crystallographic data and refinement parameters for BTF/ONA cocrystal; Table S3: Characteristic peaks in XRD patterns of BTF/ONA, BTF, and ONA; Figure S3: XRD patterns of other BTF cocrystals; Table S4: Experimental IR peak positions and transmittance (%) for BTF/ONA, BTF, and ONA; Figure S5: DSC curves of BTF/CL-20 cocrystal.

Author Contributions: Conceptualization, Y.O. and S.S.; methodology, Y.Z.; validation, Z.B.; writing—original draft preparation, S.D.; writing—review and editing, S.S.; supervision, Y.O.; funding acquisition, T.Y. All authors have read and agreed to the published version of the manuscript.

Funding: This research was funded by the National Natural Science Foundation of China (Grant No. 22305053).

Data Availability Statement: The data presented in this study are available upon request from the corresponding author.

Conflicts of Interest: The authors declare no conflicts of interest.

References

1. Akhavan, J. *The Chemistry of Explosives 4E*; Royal Society of Chemistry: London, UK, 2022; ISBN 978-1-83916-446-0.
2. Klapötke, T.M. *Chemistry of High-Energy Materials*; Walter de Gruyter GmbH & Co KG: Berlin, Germany, 2022; ISBN 978-3-11-073950-3.
3. O'Sullivan, O.T.; Zdilla, M.J. Properties and Promise of Catenated Nitrogen Systems As High-Energy-Density Materials. *Chem. Rev.* **2020**, *120*, 5682–5744. [[CrossRef](#)]
4. Belous, A.; Saladukha, V. Modern Weapons: Possibilities and Limitations. In *Viruses, Hardware and Software Trojans: Attacks and Countermeasures*; Belous, A., Saladukha, V., Eds.; Springer International Publishing: Cham, Switzerland, 2020; pp. 731–820, ISBN 978-3-030-47218-4.
5. Xu, H.; Duan, X.; Li, H.; Pei, C. A Novel High-Energetic and Good-Sensitive Cocrystal Composed of CL-20 and TATB by a Rapid Solvent/Non-Solvent Method. *RSC Adv.* **2015**, *5*, 95764–95770. [[CrossRef](#)]
6. Sun, S.; Xu, J.; Gou, H.; Zhang, Z.; Zhang, H.; Tan, Y.; Sun, J. Pressure-Induced In Situ Construction of P-CO/HNIW Explosive Composites with Excellent Laser Initiation and Detonation Performance. *ACS Appl. Mater. Interfaces* **2021**, *13*, 20718–20727. [[CrossRef](#)]
7. Kumar, N.; Dixit, A. Role of Nanotechnology in Futuristic Warfare. In *Nanotechnology for Defence Applications*; Kumar, N., Dixit, A., Eds.; Springer International Publishing: Cham, Switzerland, 2019; pp. 301–329, ISBN 978-3-030-29880-7.
8. Jiao, F.; Xiong, Y.; Li, H.; Zhang, C. Alleviating the Energy & Safety Contradiction to Construct New Low Sensitivity and Highly Energetic Materials through Crystal Engineering. *CrystEngComm* **2018**, *20*, 1757–1768. [[CrossRef](#)]

9. Wang, J.; Liu, D.; Zhang, J.; Gong, F.; Zhao, X.; Yang, Z. Design of Conductive Polymer Coating Layer for Effective Desensitization of Energetic Materials. *Chem. Eng. J.* **2024**, *482*, 148874. [[CrossRef](#)]
10. Landenberger, K.B.; Bolton, O.; Matzger, A.J. Energetic–Energetic Cocrystals of Diacetone Diperoxide (DADP): Dramatic and Divergent Sensitivity Modifications via Cocrystallization. *J. Am. Chem. Soc.* **2015**, *137*, 5074–5079. [[CrossRef](#)]
11. Foroughi, L.M.; Wiscons, R.A.; Du Bois, D.R.; Matzger, A.J. Improving Stability of the Metal-Free Primary Energetic Cyanuric Triazide (CTA) through Cocrystallization. *Chem. Commun.* **2020**, *56*, 2111–2114. [[CrossRef](#)]
12. Bellas, M.K.; Matzger, A.J. Achieving Balanced Energetics through Cocrystallization. *Angew. Chem. Int. Ed.* **2019**, *58*, 17185–17188. [[CrossRef](#)]
13. Zhang, Y.-J.; Bai, Y.; Li, J.-Z.; Fu, X.-L.; Yang, Y.-J.; Tang, Q.-F. Energetic Nitrocellulose Coating: Effective Way to Decrease Sensitivity and Modify Surface Property of HMX Particles. *J. Energetic Mater.* **2019**, *37*, 212–221. [[CrossRef](#)]
14. Zhao, X.; Zhu, W. Recent Advances in Studying the Nonnegligible Role of Noncovalent Interactions in Various Types of Energetic Molecular Crystals. *CrystEngComm* **2022**, *24*, 6119–6136. [[CrossRef](#)]
15. Baraboshkin, N.M.; Zelenov, V.P.; Minyaev, M.E.; Pivina, T.S. Quest: Structure and Properties of BTF–Nitrobenzene Cocrystals with Different Ratios of Components. *CrystEngComm* **2022**, *24*, 235–250. [[CrossRef](#)]
16. Landenberger, K.B.; Matzger, A.J. Cocrystals of 1,3,5,7-Tetranitro-1,3,5,7-Tetrazacyclooctane (HMX). *Cryst. Growth Des.* **2012**, *12*, 3603–3609. [[CrossRef](#)]
17. Bolton, O.; Matzger, A.J. Improved Stability and Smart-Material Functionality Realized in an Energetic Cocrystal. *Angew. Chem. Int. Ed.* **2011**, *50*, 8960–8963. [[CrossRef](#)]
18. Bolton, O.; Simke, L.R.; Pagoria, P.F.; Matzger, A.J. High Power Explosive with Good Sensitivity: A 2:1 Cocrystal of CL-20:HMX. *Cryst. Growth Des.* **2012**, *12*, 4311–4314. [[CrossRef](#)]
19. Satonkina, N.; Ershov, A.; Kashkarov, A.; Mikhaylov, A.; Pruel, E.; Rubtsov, I.; Spirin, I.; Titova, V. Electrical Conductivity Distribution in Detonating Benzotrifuroxane. *Sci. Rep.* **2018**, *8*, 9635. [[CrossRef](#)]
20. Suponitsky, K.Y.; Fedyanin, I.V.; Karnoukhova, V.A.; Zalomlenkov, V.A.; Gidasov, A.A.; Bakharev, V.V.; Sheremetev, A.B. Energetic Co-Crystal of a Primary Metal-Free Explosive with BTF. Ideal Pair for Co-Crystallization. *Molecules* **2021**, *26*, 7452. [[CrossRef](#)]
21. Satonkina, N.P.; Ershov, A.P. Dynamics of Carbon Nanostructures in the Benzotrifuroxan Detonation. *J. Phys. Conf. Ser.* **2021**, *1787*, 012015. [[CrossRef](#)]
22. Ji, W.; Xu, Y.; Liu, L.; Guo, C.; Wei, X.; Wang, D. The Influence of Three Binders on the Properties of BTF-Based Composite Explosive. *Cent. Eur. J. Energetic Mater.* **2023**, *20*, 369–385. [[CrossRef](#)]
23. Zhang, R.; Xia, W.; Xu, X.; Ma, P.; Ma, C. Theoretical Study on BTF-Based Cocrystals: Effect of External Electric Field. *J. Mol. Model.* **2022**, *28*, 185. [[CrossRef](#)]
24. Zhu, S.; Yang, W.; Gan, Q.; Cheng, N.; Feng, C. Early Thermal Decay of Energetic Hydrogen- and Nitro-Free Furoxan Compounds: The Case of DNTF and BTF. *Phys. Chem. Chem. Phys.* **2022**, *24*, 1520–1531. [[CrossRef](#)]
25. Zhang, H.; Guo, C.; Wang, X.; Xu, J.; He, X.; Liu, Y.; Liu, X.; Huang, H.; Sun, J. Five Energetic Cocrystals of BTF by Intermolecular Hydrogen Bond and π -Stacking Interactions. *Cryst. Growth Des.* **2013**, *13*, 679–687. [[CrossRef](#)]
26. Sen, N.; Aslan, N.; Yuksel, B.; Teciman, I. Characterization and Properties of a New Insensitive Explosive Co-Crystal Composed of Trinitrotoluene and Pyrene. *Struct. Chem.* **2024**, *35*, 553–567. [[CrossRef](#)]
27. Sultan, M.; Wu, J.; Ul Haq, I.; Imran, M.; Yang, L.; Wu, J.; Lu, J.; Chen, L. Recent Progress on Synthesis, Characterization, and Performance of Energetic Cocrystals: A Review. *Molecules* **2022**, *27*, 4775. [[CrossRef](#)]
28. Chugunova, E.A.; Timasheva, R.E.; Gibadullina, E.M.; Burirov, A.R.; Goumont, R. First Synthesis of Benzotrifuroxan at Low Temperature: Unexpected Behavior of 5,7-Dichloro-4,6-Dinitrobenzo-Furoxan with Sodium Azide. *Propellants Explos. Pyrotech.* **2012**, *37*, 390–392. [[CrossRef](#)]
29. China Ordnance Industry Standardization Research Institute. *National Military Standard of China. Experimental Methods of Sensitivity and Safety*; GJB/772A-97; State Administration of Science, Technology and Industry for National Defense: Beijing, China, 1997.
30. Reddy, L.S.; Bhatt, P.M.; Banerjee, R.; Nangia, A.; Kruger, G.J. Variable-Temperature Powder X-ray Diffraction of Aromatic Carboxylic Acid and Carboxamide Cocrystals. *Chem. Asian J.* **2007**, *2*, 505–513. [[CrossRef](#)]
31. Durga Surampudi, A.V.S.; Rajendrakumar, S.; Babu Nanubolu, J.; Balasubramanian, S.; Surov, A.O.; Voronin, A.P.; Perlovich, G.L. Influence of Crystal Packing on the Thermal Properties of Cocrystals and Cocrystal Solvates of Olanzapine: Insights from Computations. *CrystEngComm* **2020**, *22*, 6536–6558. [[CrossRef](#)]
32. Şen, N. Characterization and Properties of a New Energetic Co-Crystal Composed of Trinitrotoluene and 2,6-Diaminotoluene. *J. Mol. Struct.* **2019**, *1179*, 453–461. [[CrossRef](#)]
33. Yang, Z.; Li, H.; Zhou, X.; Zhang, C.; Huang, H.; Li, J.; Nie, F. Characterization and Properties of a Novel Energetic–Energetic Cocrystal Explosive Composed of HNIW and BTF. *Cryst. Growth Des.* **2012**, *12*, 5155–5158. [[CrossRef](#)]

34. Zhang, L.; Wu, J.-Z.; Jiang, S.-L.; Yu, Y.; Chen, J. From Intermolecular Interactions to Structures and Properties of a Novel Cocrystal Explosive: A First-Principles Study. *Phys. Chem. Chem. Phys.* **2016**, *18*, 26960–26969. [[CrossRef](#)]
35. Sun, S.; Zhang, H.; Xu, J.; Wang, H.; Wang, S.; Yu, Z.; Zhu, C.; Sun, J. Design, Preparation, Characterization and Formation Mechanism of a Novel Kinetic CL-20-Based Cocrystal. *Acta Crystallogr. Sect. B Struct. Sci. Cryst. Eng. Mater.* **2019**, *75*, 310–317. [[CrossRef](#)] [[PubMed](#)]

Disclaimer/Publisher’s Note: The statements, opinions and data contained in all publications are solely those of the individual author(s) and contributor(s) and not of MDPI and/or the editor(s). MDPI and/or the editor(s) disclaim responsibility for any injury to people or property resulting from any ideas, methods, instructions or products referred to in the content.